Value-iteration-based Adaptive Optimal Reagents Control for Antimony Flotation Process

Zhongmei Li[1], Mengzhe Huang[2], Weihua Gui[3], Zhong-ping Jiang[2]

1. School of Information Science and Engineering, East China University of Science and Technology, Shanghai 200237, P. R. China
E-mail: zhongmeili@csu.edu.cn

2. Tandon School of Engineering, New York University, Brooklyn, NY 11201,U.S.A.
E-mail: m.huang@nyu.edu,zhongping_jiang@yahoo.com

3. School of Automation, Central South University, Changsha 410083, P. R. China
E-mail: gwh@csu.edu.cn

Abstract: This paper investigates a data-driven adaptive optimal control approach for antimony flotation process in presence of input time-delay and disturbance. The integration frame of adaptive dynamic programming (ADP) and value iteration (VI) is applied to the optimal controller design without requirement of system dynamics. Fundamentally different from the existing reagents control methods, the input time-delay and disturbance are simultaneously considered in the VI-based ADP control scheme. Specifically, the disturbance is compensated directly by adding an inner model as the feedforward component to the control action and the optimal feedback gain is computed by iteratively solving Riccati equation. By exploiting industrial collected data, the numerical simulation proves that the proposed data-driven methodology can enable the concentrate and tailing grade to keep tracking the target trajectories with a minimum reagents consumption.

Key Words: Flotation process, Input time-delay, Disturbance rejection, Optimal control

1 Introduction

With the rapid development in manufacturing and "the Belt and Road" initiative, China's emerging strategic industry showing a growing appetite for antimony, rare earth, tungsten, graphite and other mineral materials. Meanwhile, much attention has been attracted to the separation technology of the above mineral resources against the background of building a community with a shared future for mining industry [1]. Flotation is a widely used, cost-effective separation technique for mineral processing, by adding certain different chemical reagents in pulp to modify the mineral hydrophobic or hydrophilic properties [2]. However, in order to obtain the desired flotation index, adjustment of reagents addition in practice are mainly relied on experienced operators, which may lead to poor flotation performance and high reagents consumption. Besides, there always exist time-delay and nonvanishing disturbance during the complex flotation process, which are not discussed in the current literature. Therefore, making stabilization and optimization of flotation processes is still a challenging that needs further investigation in order to improve the flotation performance, reduce labor intensity and reagents consumption.

To overcome the disadvantages of high arbitrariness in manual operation, several optimal control theories and strategies have been brought up for flotation reagents control problem such as the model-based approaches [3, 4], fuzzy-based or rule-based expert systems [5, 6], artificial neural networks based methods [7, 8], computer vision based control strategies [9, 10], and integration between these methods [11, 12]. Although satisfactory achievements were made in the productive practice, problems are also existed, like difficulty in model acquisition, incomplete knowledge base, weak explanation ability or poor stability. Therefore, other alternative techniques for flotation reagents control need to be carried out.

As an effective data-driven optimal control method, adaptive dynamic programming (ADP), which are sometimes called approximate dynamic programming, has been widely utilized for industrial processes for many years, because of its practical advantages such as its simple control structure, fewer tuning parameters, robustness and easy understandability [15–18]. In recent years, ADP-based control approach has been involved in the application of industrial processes, see, e.g., [19–22].

In this paper, ADP is used to find an adaptive optimal controller based on value iteration (VI) algorithm, in which the inputs time-delay and external disturbance are taken into account. The purpose of flotation reagents control is to force the flotation index to track the reference trajectories, and minimize the reagents consumption. The proposed data-driven optimal control technique has good convergence and stability which is strictly proved by rigorous proofs.

The rest of this paper is organized as follows. The working mechanism of a single flotation cell is described and the dynamic model is constructed in Section 2, which offers reliable reference for the subsequent data-driven control scheme. Section 3 provides the formation of flotation reagents control problem, and gives a data-driven control algorithm based on VI. Then, the proposed VI-based ADP algorithm is applied in the simulation of actual problem with industrial data, along with convergence analysis in Section 4. Finally, Section 5 gives some brief concluding remarks.

Notations. Throughout this paper, $\mathbf{Z}_+$ and $\mathbf{R}$ represent nonnegative integers and the set of real numbers, respectively. $vec(A) = [a_1^T, a_2^T, \cdots, a_m^T]^T$, where $a_i \in \mathbf{R}^n$ represents the ith column of $A \in \mathbf{R}^{n\times m}$. In case of $m = n$, $\lambda(A)$ denotes the set of all eigenval-

This work is supported by National Key Research and Development Project of China under Grant 2018YFB1701103, National Natural Science Foundation of China under Grant 61590922 and Grant 61533003, Natural Science Foundation of Shanghai under Grant 17ZR1406800, and the Fundamental Research Funds for the Central Universities under Grant 222201917006.

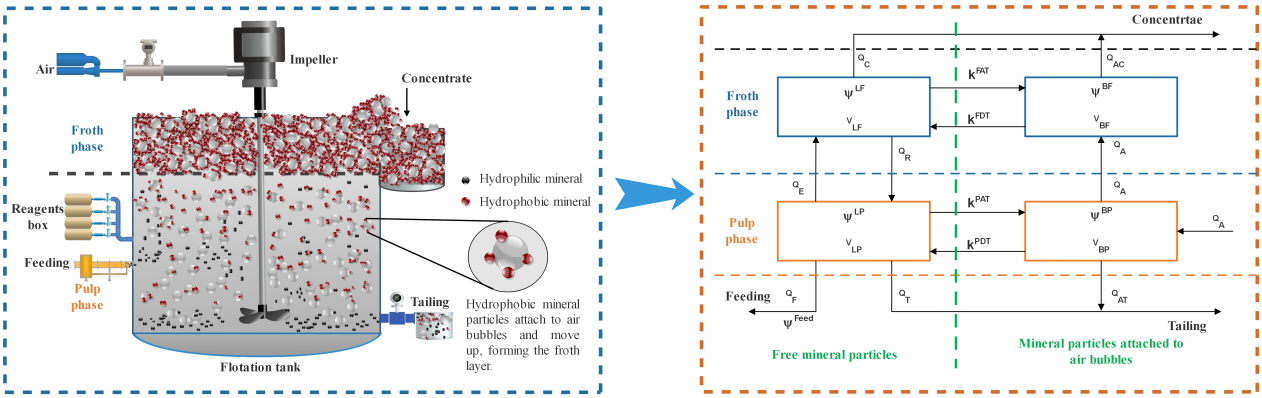

Fig. 1: The two-phase structure of a single flotation tank

ues. For a symmetric matrix $P \in \mathbf{R}^{m\times m}$, $vecs(P) = [p_{11}, 2p_{12}, \cdots, 2p_{1m}, p_{22}, 2p_{23}, \cdots, 2p_{m-1}, p_{mm}]^T \in \mathbf{R}^{\frac{1}{2}m(m+1)}$. For an arbitrary column vector $v \in \mathbf{R}^n$, $vecv(v) = [v_1^2, v_1v_2, \cdots, v_1v_n, v_2^2, \cdots, v_{n-1}v_n, v_n^2]^T \in \mathbf{R}^{\frac{1}{2}n(n+1)}$.

2 Flotation Process Description

The antimony flotation process consists of a rougher cell, two cleaner cells and two scavenger cells. Since the reagents addition is completed in the rougher circuit, and the final concentrate/tailing products are respectively obtained through the cleaner circuit and scavenger circuit separation. Therefore, the "rougher-cleaner-scavenger" circuits can be condensed into a single flotation tank for analyzing the antimony flotation process which can be seen in Fig. 1.

The flotation tank is equipped with an impeller at the bottom so as to agitate the flotation pulp, as shown in Fig. 1. The flotation cell can be divided into two phases based on the maldistribution of mineral particles: froth phase and pulp phase. Both phases are vulnerable to chemical reagents. After feeding and reagents are added to the pulp phase, the useful minerals with hydrophobic property attach to air bubbles, which move upward and form the froth layer at the top of flotation cell. The valuable minerals in the froth layer are scraped from the flotation tank, known as the concentrate product. Meanwhile, the hydrophilic minerals remain in the pulp, and are drained off along with underflow, which forms the tailing product.

The flotation performance is usually assessed in terms of tailing and concentrate grade. In practice, the tailing and concentrate grade are determined by the air flow rate, impeller speed, feeding grade and chemical reagents (PH value, frother, activator and collector). In our experiment, air flow rate and impeller speed are fixed, and the feeding grade is identified by X-ray fluorescence analyzer. To meet the production requirement, it is possible to modify reagents addition to selectively changing mineral surface characteristics.

2.1 Modeling the antimony flotation process

From flotation process mechanism, there exists four states of mineral particles in the flotation cell which can be seen in Fig. 1. Based on [23], the dynamic relationship can be modeled based on the flotation dynamics and mass balance model:

(1). Free mineral particles in pulp phase

$$\frac{\mathrm{d}}{\mathrm{dt}}(V_{\mathrm{LP}}\psi^{\mathrm{LP}}) = -k^{\mathrm{PAT}}V_{\mathrm{LP}}\psi^{\mathrm{LP}} + k^{\mathrm{PDT}}V_{\mathrm{BP}}\psi^{\mathrm{BP}} + Q_{\mathrm{Feed}}\psi^{\mathrm{Feed}} - Q_{\mathrm{T}}\psi^{\mathrm{LP}} + Q_{\mathrm{R}}k^{\mathrm{R}}\psi^{\mathrm{LF}} - Q_{\mathrm{E}}\psi^{\mathrm{LP}}. \quad (1)$$

(2). Mineral particles attached to air bubbles in pulp phase

$$\frac{\mathrm{d}}{\mathrm{dt}}(V_{\mathrm{BP}}\psi^{\mathrm{BP}}) = -k^{\mathrm{PDT}}V_{\mathrm{BP}}\psi^{\mathrm{BP}} + k^{\mathrm{PAT}}V_{\mathrm{LP}}\psi^{\mathrm{LP}} - Q_{\mathrm{A}}\psi^{\mathrm{BP}} + Q_{\mathrm{AT}}\psi^{\mathrm{BP}}. \quad (2)$$

(3). Free mineral particles in froth phase

$$\frac{\mathrm{d}}{\mathrm{dt}}(V_{\mathrm{LF}}\psi^{\mathrm{LF}}) = -k^{\mathrm{FAT}}V_{\mathrm{LF}}\psi^{\mathrm{LF}} + k^{\mathrm{FDT}}V_{\mathrm{BF}}\psi^{\mathrm{BF}} - Q_{\mathrm{E}}\psi^{\mathrm{LP}} - Q_{\mathrm{R}}k^{\mathrm{R}}\psi^{\mathrm{LF}} - Q_{\mathrm{C}}\psi^{\mathrm{LF}}. \quad (3)$$

(4). Mineral particles attached to air bubbles in froth phase

$$\frac{\mathrm{d}}{\mathrm{dt}}(V_{\mathrm{BF}}\psi^{\mathrm{BF}}) = -k^{\mathrm{FDT}}V_{\mathrm{BF}}\psi^{\mathrm{BF}} + k^{\mathrm{FAT}}V_{\mathrm{LF}}\psi^{\mathrm{LF}} + Q_{\mathrm{A}}\psi^{\mathrm{BP}} - Q_{\mathrm{AC}}\psi^{\mathrm{BF}}. \quad (4)$$

where ψ represents the number of mineral particles in the corresponding state, V_{LP} is the pulp volume in pulp phase, V_{BP} is the gas volume in pulp phase, V_{LF} is the pulp volume in froth phase, V_{BF} is the gas volume in froth phase, k^{FAT} is the attachment rate constant of mineral particles-bubbles in froth phase, k^{FDT} is the detachment rate constant of mineral particles and bubbles in froth phase, k^{PAT} is the attachment rate constant of mineral particles-bubbles in pulp phase, k^{PDT} is the detachment rate constant of mineral particles and bubbles in pulp phase, Q_{Feed} is the feeding flow rate, Q_T is the tailing flow rate, Q_{C} is the concentrate flow rate, Q_{R} is the flow rate of falling mineral particles from froth phase to pulp phase, k^{R} is the flow rate constant of falling mineral particles from froth phase to pulp phase, Q_{E} is the flow rate of entrained mineral particles from pulp phase to froth phase, Q_{A} is air flow rate, Q_{AT} is the air flow rate from pulp phase to tailing, Q_{AC} is the air flow rate from froth phase to concentrate, V is the flotation cell volume, V_{TF} is the volume of froth phase, V_{TP} is the volume of pulp phase.

Equation (1)-(4) can be rewritten as follows by separately adding up the mineral particles in froth phase and pulp phase (free and attached to air bubbles)

Pulp phase:

$$\frac{\mathrm{d}}{\mathrm{dt}}(V_{\mathrm{LP}}\psi^{\mathrm{LP}} + V_{\mathrm{BP}}\psi^{\mathrm{BP}}) = Q_{\mathrm{Feed}} - Q_{\mathrm{T}}\psi^{\mathrm{LP}} + Q_{\mathrm{R}}k^{\mathrm{R}}\psi^{\mathrm{LF}} - Q_{\mathrm{E}}\psi^{\mathrm{LP}} - Q_{\mathrm{A}}\psi^{\mathrm{BP}} + Q_{\mathrm{AT}}\psi^{\mathrm{BP}}. \quad (5)$$

Froth phase:

$$\frac{\mathrm{d}}{\mathrm{dt}}(V_{\mathrm{LF}}\psi^{\mathrm{LF}} + V_{\mathrm{BF}}\psi^{\mathrm{BF}}) = -Q_{\mathrm{E}}\psi^{\mathrm{LP}} - Q_{\mathrm{R}}k^{\mathrm{R}}\psi^{\mathrm{LF}} - Q_{\mathrm{C}}\psi^{\mathrm{LF}} + Q_{\mathrm{A}}\psi^{\mathrm{BP}} - Q_{\mathrm{AC}}\psi^{\mathrm{BF}}. \quad (6)$$

Suppose there is a physical equilibrium between mineral particles attached to bubbles and free particles:

$$\psi^{\mathrm{BP}} = \alpha_{\mathrm{P}}\frac{V_{\mathrm{LP}}}{V_{\mathrm{BP}}}\psi^{\mathrm{LP}}, \quad (7)$$

$$\psi^{\mathrm{BF}} = \alpha_{\mathrm{F}}\frac{V_{\mathrm{LP}}}{V_{\mathrm{BP}}}\psi^{\mathrm{LF}}. \quad (8)$$

The number of particles per unit volume in pulp phase can be represented by

$$\psi^{\mathrm{MP}} = \psi^{\mathrm{LP}} + \frac{V_{\mathrm{BP}}}{V_{\mathrm{LP}}}\psi^{\mathrm{BP}}. \quad (9)$$

Substituting (7) into (9)

$$\psi^{\mathrm{MP}} = (1+\alpha_{\mathrm{P}})\psi^{\mathrm{LP}} \quad (10)$$

Similarly, the number of particles per unit volume in froth phase can be written as

$$\psi^{\mathrm{MF}} = (1+\alpha_{\mathrm{F}})\psi^{\mathrm{LF}}. \quad (11)$$

Substituting (7), (8), (10), (11) into (5) and (6), we have

$$\frac{\mathrm{d}}{\mathrm{dt}}(V_{\mathrm{LP}}\psi^{\mathrm{MP}}) = Q_{\mathrm{Feed}}\psi^{\mathrm{Feed}} - (Q_{\mathrm{T}} + Q_{\mathrm{E}} + Q_{\mathrm{A}}\alpha_{\mathrm{P}}\frac{V_{\mathrm{LP}}}{V_{\mathrm{BP}}} + Q_{\mathrm{T}}\alpha_{\mathrm{P}})\frac{\psi^{\mathrm{MP}}}{(1+\alpha_{\mathrm{P}})}, \quad (12)$$

$$\frac{\mathrm{d}}{\mathrm{dt}}(V_{\mathrm{LF}}\psi^{\mathrm{MF}}) = (Q_{\mathrm{A}}\alpha_{\mathrm{P}}\frac{V_{\mathrm{LP}}}{V_{\mathrm{BP}}} + Q_{\mathrm{E}})\frac{\psi^{\mathrm{MP}}}{(1+\alpha_{\mathrm{P}})} - (Q_{\mathrm{R}}k^{\mathrm{R}} + Q_{\mathrm{C}}(1+\alpha_{\mathrm{F}}))\frac{\psi^{\mathrm{MF}}}{1+\alpha_{\mathrm{F}}}. \quad (13)$$

To simplify the model, the following assumptions are made:

(1). The mineral particles are completely mixed with the air bubbles in pulp phase;

(2). The mineral particles are completely mixed with the air bubbles in froth phase;

(3). The mineral particles are uniform in size and shape;

(4). In steady state, $Q_{\mathrm{A}} = Q_{\mathrm{AC}} + Q_{\mathrm{AT}}$;

(5). $Q_{\mathrm{C}}/Q_{\mathrm{AC}} = V_{\mathrm{LF}}/V_{\mathrm{BF}}$, $Q_{\mathrm{T}}/Q_{\mathrm{AT}} = V_{\mathrm{LP}}/V_{\mathrm{BP}}$.

Based on the assumption, (12) and (13) can be rewritten as

$$\frac{\mathrm{dC}^{\mathrm{MP}}}{\mathrm{dt}} = \frac{Q_{\mathrm{Feed}}C^{\mathrm{Feed}}}{V_{\mathrm{LP}}} - \frac{(Q_{\mathrm{E}} + Q_{\mathrm{A}}\alpha^{\mathrm{P}}V_{\mathrm{LP}}/V_{\mathrm{BP}})}{(1+\alpha^{\mathrm{P}})V_{\mathrm{LP}}}C^{\mathrm{MP}} + \frac{Q_{\mathrm{R}}k^{\mathrm{R}}C^{\mathrm{MF}}}{(1+\alpha^{\mathrm{F}})V_{\mathrm{LP}}} - \frac{Q_{\mathrm{T}}C^{\mathrm{MP}}}{(1+\alpha^{\mathrm{P}})V_{\mathrm{LP}}}, \quad (14)$$

$$\frac{\mathrm{dC}^{\mathrm{MF}}}{\mathrm{dt}} = \frac{(Q_{\mathrm{E}} + Q_{\mathrm{A}}\alpha^{\mathrm{P}}V_{\mathrm{LP}}/V_{\mathrm{BP}})}{(1+\alpha^{\mathrm{P}})V_{\mathrm{LF}}}C^{\mathrm{MP}} - \frac{Q_{\mathrm{R}}k^{\mathrm{R}}C^{\mathrm{MF}}}{(1+\alpha^{\mathrm{F}})V_{\mathrm{LF}}} - \frac{Q_{\mathrm{C}}C^{\mathrm{MF}}}{V_{\mathrm{LF}}}. \quad (15)$$

Note that (14) and (15) represents mineral mass balance in pulp phase and froth phase, respectively.

In order to establish the relationship between reagents addition and flotation indexes, define the tailing grade

$$R_1 = \frac{C^{\mathrm{MP}}Q_{\mathrm{T}}}{V_{\mathrm{LP}}C^{\mathrm{Feed}}Q_{\mathrm{Feed}}}, \quad (16)$$

and the concentrate

$$R_2 = \frac{C^{\mathrm{MP}}Q_{\mathrm{T}}}{V_{\mathrm{LP}}C^{\mathrm{Feed}}Q_{\mathrm{Feed}}}. \quad (17)$$

Substitute (16) and (17) into (14) and (15)

$$\frac{\mathrm{dR}_1}{\mathrm{dt}} = \frac{Q^{\mathrm{T}}}{V_{\mathrm{LP}}^2} - \frac{(Q_{\mathrm{E}} + Q_{\mathrm{A}}\alpha^{\mathrm{P}}V_{\mathrm{LP}}/V_{\mathrm{BP}})}{(1+\alpha^{\mathrm{P}})V_{\mathrm{LP}}}R_1 + \frac{Q_{\mathrm{R}}k^{\mathrm{R}}V_{\mathrm{LF}}}{(1+\alpha^{\mathrm{F}})V_{\mathrm{LP}}}\frac{Q_{\mathrm{T}}Q_{\mathrm{C}}}{V_{\mathrm{LP}}}R_2 - \frac{Q_{\mathrm{T}}}{(1+\alpha^{\mathrm{P}})V_{\mathrm{LP}}}R_1, \quad (18)$$

$$\frac{\mathrm{dR}_2}{\mathrm{dt}} = \frac{(Q_{\mathrm{E}} + Q_{\mathrm{A}}\alpha^{\mathrm{P}}V_{\mathrm{LP}}/V_{\mathrm{BP}})}{(1+\alpha^{\mathrm{P}})V_{\mathrm{LF}}}\frac{Q_{\mathrm{C}}}{Q_{\mathrm{T}}}R_1 - \frac{Q_{\mathrm{R}}k^{\mathrm{R}}}{(1+\alpha^{\mathrm{F}})V_{\mathrm{LP}}}R_2 - \frac{Q_{\mathrm{C}}}{V_{\mathrm{LP}}}R_2, \quad (19)$$

where $V_{\mathrm{TF}} = V_{\mathrm{BF}} + V_{\mathrm{LF}}$, $V_{\mathrm{TP}} = V_{\mathrm{BP}} + V_{\mathrm{LP}}$.

To analyze the optimal control problem, the model was modified to study the effect of operation variables on flotation performance. Based on [24]

$$Q_{\mathrm{E}} = \frac{6\delta}{d_{\mathrm{BP}}}Q_{\mathrm{air}} = r_1 Q_{\mathrm{A}}, \quad (20)$$

$$Q_{\mathrm{R}} = \frac{1-\mu_{\mathrm{F}}}{\mu_{\mathrm{F}}}\frac{Q_{\mathrm{air}}}{S} = r_2 Q_{\mathrm{A}}, \quad (21)$$

where δ is the thickness of the film around air bubble, d_{BP} is mean bubble diameter in pulp phase, μ_{F} is the average gas content in the froth phase, r_1 and r_2 are variables that vary with the operating conditions.

Equation (18) and (19) retain the essential characteristics of (1) and (4), which draw a distinction of mineral particles-bubbles attachment/detachment mechanism between pulp phase and froth phase. Q_{A}, Q_{T}, and Q_{C} in practice are usually first adjusted to a reasonable value and rarely manipulated during production. Therefore, the unknown parameters in the model is the attachment/detachment rate constant α^{F} of mineral particles-bubbles in the froth phase, the attachment/detachment rate constant α^{P} in the pulp phase, and the falling back rate constant k^{R}. All these parameters are affected by the reagents addition.

Empirically, the PH value O_1 affects mineral floatability by changing the mineral surface properties in the pulp phase. We can assume that α^{P} is related to O_1 with proportion relationship based on [25] and [26]. Besides, α^{P} is associated with collector flow rate O_2, because collector promotes the hydrophobic properties of useful minerals and facilitates the

attachment of mineral particles to bubbles. As O_2 increases, α^{P} grows in a suitable range [27]. Therefore, it can be assumed that

$$\alpha^{\mathrm{P}} = m_1 O_1 O_2. \tag{22}$$

α^{F} and k^{R} are mainly affected by bubble residence time, which is related to activator and frother. Because the bubble viscosity increases with the increase of activator flow rate O_3 and frother flow rate O_4, which causes the bubble residence time in froth phase increases. Thus, it becomes difficult for the valuable minerals to fall back, which affects the final tailing grade and concentrate grade [28, 29]. Assume

$$\alpha^{\mathrm{F}} = m_2 O_3 O_4, \tag{23}$$

$$k^{\mathrm{R}} = m_3 O_3 + m_4 O_4 + m_5. \tag{24}$$

Hence, the dynamic model between flotation indexes and chemical reagents can be deduced, which lays a foundation for establishing the simulation environment for the subsequent data-driven optimal reagents control methods. (18) and (19) become

$$\begin{aligned}\frac{\mathrm{dR}_1}{\mathrm{dt}} = &-[\frac{(r_1 Q_{\mathrm{A}} + Q_{\mathrm{A}} m_1 O_1 O_2)}{(1+m_1 O_1 O_2) V_{\mathrm{LP}} V_{\mathrm{BP}}} + \frac{Q_{\mathrm{T}}}{(1+m_1 O_1 O_2) V_{\mathrm{LP}}}] R_1 \\ &+ \frac{Q^{\mathrm{T}}}{V_{\mathrm{LP}}^2} + \frac{r_2 Q_{\mathrm{A}} (m_3 O_3 + m_4 O_4 + m_5) V_{\mathrm{LF}}}{(1+m_1 O_1 O_2) V_{\mathrm{LP}}} \frac{Q_{\mathrm{T}} Q_{\mathrm{C}}}{V_{\mathrm{LP}}} R_2,\end{aligned} \tag{25}$$

$$\begin{aligned}\frac{\mathrm{dR}_2}{\mathrm{dt}} = &\frac{(r_1 Q_{\mathrm{A}} + Q_{\mathrm{A}} m_1 O_1 O_2 V_{\mathrm{LP}}/V_{\mathrm{BP}})}{(1+m_1 O_1 O_2) V_{\mathrm{LF}}} \frac{Q_{\mathrm{C}}}{Q_{\mathrm{T}}} R_1 \\ &- \frac{r_2 Q_{\mathrm{A}} (m_3 O_3 + m_4 O_4 + m_5)}{(1+m_2 O_3 O_4) V_{\mathrm{LP}}} R_2 - \frac{Q_{\mathrm{C}}}{V_{\mathrm{LP}}} R_2,\end{aligned} \tag{26}$$

where m_1, m_2, m_3, m_4, m_5, r_1 and r_2 are parameters to be identified. The behavior of particles-bubble in the pulp phase and froth phase can be influenced by optimizing the reagents addition PH value O_1, collector flow rate O_2, activator flow rate O_3 and frother flow rate O_4, which is essential to mineral recovery.

3 Flotation reagents control problem with input time-delay

To address the reagents control problem during antimony flotation process which is defined in the previous section, a data-driven adaptive optimal control strategy is examined in this section. The objective is to make tailings grade and concentrate grade satisfy the production requirements and keep the reagents consumption to a minimum.

3.1 Reagents control problem description

By defining

$$x_1 = R_1 - R_{1\mathrm{eq}}, \tag{27}$$

$$x_2 = R_2 - R_{2\mathrm{eq}}, \tag{28}$$

where R_1 represents the tailing grade, R_2 denotes the concentrate grade, $R_{1\mathrm{eq}}$ and $R_{2\mathrm{eq}}$ are the ideal values of tailing grade and concentrate grade, respectively. x_1 and x_2 are tracking errors.

The flotation process model defined in Section 2 can be expresses as

$$\dot{x} = A_c x + \sum_{i=1}^{4} B_{ci} \mu(t - \tau_i) + D_c, \tag{29}$$

in which $x = [x_1, x_2]^T \in \mathbf{R}^n$ is the system state vector that needs to be tracked, $\mu = [\mu_1, \mu_2, \mu_3, \mu_4]^T = [O_1, O_2, O_3, O_4]^T \in \mathbf{R}^m$ is control input, D_c represents disturbance. $A_c \in \mathbf{R}^{n\times n}$, $B_{ci} \in \mathbf{R}^{n\times m}$, $D_c \in \mathbf{R}^n$, τ_i is the input time-delay, and

$$\tau_i = (d_i - 1)h + \tau_i^{'}, \tag{30}$$

where d_i is a given integer, $i = 1, 2, 3, 4$ satisfies $1 \le d_1 \le d_2 \le d_3 \le d_4$, h is the sampling period, $0 < \tau_i^{'} \le h$.

Based on [30], the flotation process model (29) can be discretized into

$$\begin{aligned}x(kh+h) &= e^{A_c h} x(kh) + \int_{kh}^{(kh+h)} e^{A_c(kh+h-s^{'})} D_c ds^{'} \\ &+ \sum_{i=1}^{4} \int_{kh}^{(kh+h)} e^{A_c(kh+h-s^{'})} B_{ci} \mu(s^{'} - \tau_i) ds^{'} \\ &= Mx(kh) + E_d \\ &+ \sum_{i=1}^{4} [\Gamma_{0i} u(kh - d_i h) + \Gamma_{1i} u(kh - (d_i - 1)h)],\end{aligned} \tag{31}$$

where $M = e^{A_c h}$, $\Gamma_{0i} = e^{A_c(h-\tau_i{'})} \int_0^{\tau_i^{'}} e^{A_c s} ds B_{ci}$, $\Gamma_{1i} = \int_0^{h-\tau_i^{'}} e^{A_c s} ds B_{ci}$, $E_d = \int_{kh}^{(kh+h)} e^{A_c(kh+h-s^{'})} D_c ds^{'}$.

Define $\xi_k = [x^T(k), u^T(k-d_4), u^T(k-d_4+1), \cdots, u^T(k-1)]^T \in \mathbf{R}^q$, $q = n + md_4$. System (31) can be written as:

$$\xi_{k+1} = H_d \xi_k + G_d u_k + E_d, \tag{32}$$

in which H_d and G_d are described by

$$H_d = \begin{bmatrix} \Phi & \Gamma_{0i} & \Gamma_{1i} & \cdots & 0 \\ 0 & 0 & I_m & \cdots & 0 \\ \vdots & \vdots & \vdots & \ddots & \vdots \\ 0 & 0 & 0 & \cdots & I_m \\ 0 & 0 & 0 & \cdots & 0 \end{bmatrix}, G_d = \begin{bmatrix} 0 \\ 0 \\ \vdots \\ 0 \\ I_m \end{bmatrix}.$$

First, define an internal model v to reject the external disturbance based on [31]

$$v_{k+1} = v_k + x_k. \tag{33}$$

Define $z_k = [\xi_k^T, v_k^T]^T$, one has

$$z_{k+1} = A_d z_k + B_d u_k + D_d, \tag{34}$$

and

$$x_k = C_d z_k, \tag{35}$$

in which $A_d = \begin{bmatrix} H_d & 0 \\ C & I_2 \end{bmatrix}$, $B_d = \begin{bmatrix} G_d \\ 0 \end{bmatrix}$, $D_d = \begin{bmatrix} E_d \\ 0 \end{bmatrix}$, $C_d = \begin{bmatrix} I_n & 0_{n\times(n_z-n)} \end{bmatrix}$, $n_z = q + n$.

Theorem 1. *Given a matrix $K = \begin{bmatrix} K_\xi & K_v \end{bmatrix} \in \boldsymbol{R}^{m\times n_z}$ makes all of the eigenvalues of $A_d - B_d K$ are in the unit circle. The controller can be designed as $u_k = -K z_k$. Then, according to* (34)*, we have $\lim_{k\to\infty} x_k = 0$, the asymptotic tracking problem with input time-delay and disturbance is solved.*

Proof. According to [31, Lemma 1.37], there exists an optimal feedback gain K. The closed-loop system can be expressed as

$$z_{k+1} = (A_d - B_d K) z_k + D_d. \tag{36}$$

Then, we define the stable state z^*

$$\begin{aligned} z^* &= [I_{n_z} - (A_d - B_d K)]^{-1} D_d \\ &= [\xi^*, v^*]^T, \end{aligned} \tag{37}$$

where v^* is the steady state value of the compensator v, which is determined by K.

$$K_\epsilon = (B_d^T P_{j+1} B_d + R)^{-1} B_d^T P_{j+1} A_d \tag{38}$$

in which $P_j = A_d^T P_{j+1}(A_d - B_d K_\epsilon) + Q$. The disturbance term compensator

$$v_k = (A_d - B_d K_\epsilon)^T v_{k+1} - (A_d - B_d K_\epsilon)^T P_{k+1} E_d \tag{39}$$

and the corresponding control gain

$$K_v = (B_d^T P_{j+1} B_d + R)^{-1} B_d^T. \tag{40}$$

Therefore, the controller is

$$u_k = K_\epsilon z_k + K_v v_{k+1}. \tag{41}$$

Let $K = \begin{bmatrix} K_\epsilon & K_v \end{bmatrix}$, the steady-state input is $u^* = -Kz^*$.

Next, define the state tracking error and input error as $\bar{z}_k = z_k - z^*$, $\bar{u}_k = u_k - u^*$, respectively. According to (36), we have

$$\begin{aligned} \bar{z}_{k+1} &= A_d \bar{z}_k + B_d \bar{u}_k + (A_d - I_{n_z}) z^* + B_d u^* + D_d \\ &= (A_d - B_d K) \bar{z}_k. \end{aligned} \tag{42}$$

Because $A_d - B_d K$ is a Schur matrix, one can check that $\lim_{k\to\infty} \bar{z}_k = 0$, which means $\lim_{k\to\infty} z_k = z^*$, $\lim_{k\to\infty} x_k = x^* = 0$, $\lim_{k\to\infty} u_k = u^*$. Thus, the stability of the closed-loop system is guaranteed. ■

According to the above analysis, the objective of flotation reagents optimal control problem is to find a control strategy that forces the tracking error z_k to converge to zero with a minimum reagents consumption O_1-O_4 while the disturbance D_d and input time-delay τ_i exist. Note that the compensator v is an essential step to realize the asymptotic tracking of tailing grade and concentrate grade during flotation process.

The reagents control problem can be represented as the following optimal control problem, also known as linear quadratic regulator (LQR) problem:

$$\begin{aligned} \min_{\bar{u}} \quad & \sum_{k=0}^{\infty} \bar{z}_k^T Q \bar{z}_k + \bar{u}_k^T R \bar{u}_k \\ \text{subject to} \quad & \bar{z}_{k+1} = A_d \bar{z}_k + B_d \bar{u}_k, \end{aligned}$$

where $Q = Q^T > 0$, $R > 0$, $(A_d, \sqrt{Q})$ is observable. The target is to find the optimal feedback gain K^* by calculating LQR problem, and design a controller $\bar{u}_k = -K^* \bar{z}_k$. Thus, the asymptotic tracking of the closed-loop system (34) is realized.

According to linear optimal control theory [32], $P^* = P^{*T} > 0$ is the unique solution for the following Algebra Riccati Equation (ARE):

$$A_d^T P_j A_d - P_j + Q - A_d^T P_j B_d \left(R + B_d^T P_j B_d\right)^{-1} B_d^T P_j A_d = 0. \tag{43}$$

K^* can be solved by the following equation

$$K^* = \left(R + B_d^T P_j B_d\right)^{-1} B_d^T P^* A_d. \tag{44}$$

However, P in DARE (43) is nonlinear, which is generally difficult to solve directly. The value iteration (VI) algorithm can be used to get an approximate solution of (43).

Algorithm 1 VI Algorithm

1: Choose a small enough constant $\epsilon > 0$, $j \leftarrow 0$, $P_j \leftarrow 0$.
2: **repeat**
3: Calculate P_{j+1} and K_{j+1} by the following equation

$$P_{j+1} \leftarrow A_d^T P_j A_d + Q - A_d^T P_j B_d (R_d + B_d^T P_j B_d)^{-1} B_d^T P_j A_d \tag{45}$$

$$K_{j+1} \leftarrow (R + B_d^T P_{j+1} B_d)^{-1} B_d^T P_{j+1} A_d \tag{46}$$

4: $j \leftarrow j + 1$
5: **until** $|P_j - P_{j-1}| < \epsilon$.

Remark 1. *Considering P_j and K_j defined in* (45) *and* (46)*, for all sequences $\{P_j\}_{j=1}^{\infty}$ and $\{K_j\}_{j=1}^{\infty}$, it has*

(1). $\lim_{j\to\infty} K_j = K^*$

(2). $\lim_{j\to\infty} P_j = P^*$

[33] has proved the convergence of this model-based control method. The model-based controller design procedure is given in Algorithm 1, from which we can get the optimal feedback gain K^* based on (45)-(46).

Obviously, the system coefficient matrices A_d, B_d, and D_d are required if the model-based approach is employed. However, it is costly to identify an accurate system model because of the complexity and large time delay of the actual flotation process. Therefore, a data-driven adaptive optimal control method is proposed to solve the reagents control problem in the presence of input time-delay and disturbance.

3.2 Data-Driven ADP controller design

The purpose for the flotation reagents control problem is to design an optimal controller, so as to enable the system state x to track the target value, and keep the reagents consumption u to a minimum. This paper presents a VI-based ADP algorithm to find the optimal control strategy with online measurement data, and the control structure is shown in Fig. 2, where Z^{-1} is delay operator. The real-time tailing and concentrate grade are measured online. ξ_k supplies the current system state x and the historical input u. The feedback gain K is calculated by using the VI-based ADP algorithm with v_k functions as a compensator, which facilitate the tailing grade R_1 and concentrate grade R_2 tracking the target values $R_{eq} = [R_{1eq}, R_{2eq}]^T$ with a small tracking error $x = [x_1, x_2]^T$.

System (34) can be written as

$$z_{k+1} = A_j z_k + B_d(K_j z_k + u_k) + D_d, \tag{47}$$

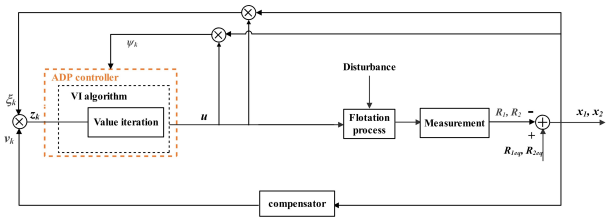

Fig. 2: Reagents control structure under ADP controller

in which $A_j = A_d - B_d K_j$.

A data-driven VI-based ADP controller design method is given, in which it starts with a random function, then find an improved function during the iteration until the optimal one is chosen.

Defining the following matrix:

$$\begin{aligned} H_j &= \begin{bmatrix} H_j^{11} & H_j^{12} & H_j^{13} \\ \left(H_j^{11}\right)^T & H_j^{22} & H_j^{23} \\ \left(H_j^{13}\right)^T & \left(H_j^{23}\right)^T & H_j^{33} \end{bmatrix} \\ &:= \begin{bmatrix} B_d^T P_j B_d & B_d^T P_j D_d & B_d^T P_j A_d \\ D_d^T P_j B_d & D_d^T P_j A_d & D_d^T P_j A_d \\ A_d^T P_j B_d & A_d^T P_j D_d & A_d^T P_j A_d \end{bmatrix}. \end{aligned}$$

By (45) and (47), the VI equation can be written as

$$\begin{aligned} & z_{k+1}^T Q z_{k+1} \\ =& - z_{k+1}^T \mathcal{F}(P_j) z_{k+1} + z_{k+1}^T P_{j+1} z_{k+1} \\ =& - z_{k+1}^T \left[H_j^{33} - (H_j^{13})^T (R + H_j^{11})^{-1} H_j^{13}\right] z_{k+1} \\ & + \left(\begin{bmatrix} u_k \\ 1 \\ z_k \end{bmatrix} \otimes \begin{bmatrix} u_k \\ 1 \\ z_k \end{bmatrix} \right)^T \mathrm{vec}(H_{j+1}) \\ =& z_{k+1}^T \left[H_j^{33} - (H_j^{13})^T (R + H_j^{11})^{-1} H_j^{13}\right] z_{k+1} \\ & + \left[\mathrm{vecv} \left(\begin{bmatrix} u_k \\ 1 \\ z_k \end{bmatrix} \right) \right]^T \mathrm{vecs}(H_{j+1}) \\ =& - \phi_{k+1}^j + \psi_k^T \mathrm{vecs}(H_{j+1}), \end{aligned} \tag{48}$$

where

$\mathcal{F}(P_j) = A_d^T P_j A_d - A_d^T P_j B_d \left(R + B_d^T P_j B_d\right)^{-1} B_d^T P_j A_d$,

$\phi_{k+1}^j = -z_{k+1}^T \left[H_j^{33} - \left(H_j^{13}\right)^T \left(R + H_j^{11}\right)^{-1} H_j^{13}\right] z_{k+1}$,

$\psi_k = vecv\left(\begin{bmatrix} u_k^T & 1 & z_k^T \end{bmatrix}^T\right)$, $\otimes$ is Kronecker product.

Algorithm 2 VI-based ADP algorithm for flotation reagents control problem

1: Find a small enough constant $\epsilon > 0$.
2: Given an initial control policy u_k in $[0, k_{0,0})$, $j \leftarrow 0$, $H_j \leftarrow 0$, $K_j \leftarrow 0$.
3: **repeat**
4: Employ control strategy $u_k^j = -K_j z_k + e_k$ in $[k_{j,0}, k_{j,s}]$.
5: Solve H_{j+1} through (49)
6: $K_{j+1} \leftarrow (R + H_{j+1}^{11})^{-1} H_{j+1}^{13}$
7: $j \leftarrow j + 1$
8: **until** $|H_j - H_{j-1}| < \epsilon$.

For any sampling instant $k \in \mathbf{Z}_+$, (48) holds. In order to find out H_{j+1}, z and u are collected within $k_0 < k_1 < \cdots < k_N$, in which N is a big enough integer.

By defining $\psi_V = [\psi_{k0}, \psi_{k1}, \cdots, \psi_{ks}]^T$, $\Phi_j^V = [z_{k_0+1}^T Q z_{k_0+1} + \phi_{k0+1}^j, z_{k_1+1}^T Q z_{k_1+1} + \phi_{k_1+1}^j, \cdots, z_{k_s+1}^T Q z_{k_s+1} + \phi_{k_s+1}^j]^T$.

(48) can be expressed as

$$\psi_V vecs\left(H_{j+1}\right) = \Phi_j^V . \tag{49}$$

Assumption 1. *There exists a positive integer $s_0 \in \mathbf{Z}_+$, for any $s > s_0$, ψ_V is full of rank.*

Remark 2. *In order to make the Assumption 1 holds, let $u_k = -K_0 z_k + e_k$ as control input, in which e_k is exploration noise [34].*

Under Assumption 1, we obtain the unique solution to (49) via the least square method

$$vecs(H_{j+1}) = (\psi_V^T \psi_V)^{-1} \psi_V^T \Phi_j^V . \tag{50}$$

Therefore, the optimal feedback gain K_{j+1} can be updated through (50)

$$K_{j+1} = \left(R + H_j^{11}\right)^{-1} \left(H_j^{13}\right). \tag{51}$$

Finally, the flotation reagents control method based on ADP is given in Algorithm 2, which only require the system input and state information instead of the flotation mathematical model.

The following theorem shows the convergence of Algorithm 2.

Theorem 2. *Under Assumption 1 and the proposed VI-based ADP Algorithm 2, it can be known that:*
(1). $\lim_{j \to \infty} H_j = H_d^*$;
(2). $\lim_{j \to \infty} K_j = K_d^*$.
where $H_d^* = \begin{bmatrix} B_d^T P_d^* B_d & B_d^T P_d^* D_d & B_d^T P_d^* A_d \\ D_d^T P_d^* B_d & D_d^T P_d^* A_d & D_d^T P_d^* A_d \\ A_d^T P_d^* B_d & A_d^T P_d^* D_d & A_d^T P_d^* A_d \end{bmatrix}$.

Proof. If P_{j+1} is the solution of (45), the unique solution H_{j+1} can be obtained. Based on (48), it can be clearly see that H_{j+1} satisfies (50). Let H be the solution of (50), we have $H = H_{j+1}$ because ψ_V is full of rank, which means the least squares solution of (50) is equivalent to the solution of Algorithm 1. Therefore, the convergence of H_{j+1} and K_{j+1} is proved. ■

Then, the following theorem shows the local stability of the proposed VI-based ADP control method.

Theorem 3. *Employing the control strategy K_{j^*} iteratively obtained by Algorithm 2, the flotation performance reaches the target value, i.e.,* $\lim_{k \to \infty} x_k = 0$.

Proof. According to Theorem 2, $A_d - B_d K_{j^*}$ is a Schur matrix, employ the optimal controller learned from VI-based ADP algorithm to the closed-loop system, which satisfies

$$\bar{z}_{k+1} = (A_d - B_d K_{j^*}) \bar{z}_k. \tag{52}$$

Based on Theorem 1, one can check that $\lim_{k \to \infty} x_k = 0$. ■

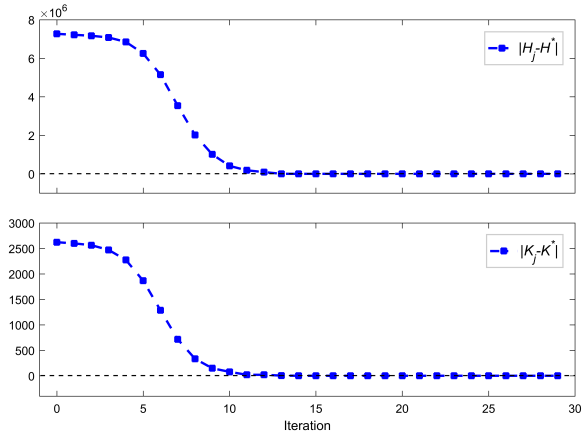

Fig. 3: H_j and K_j compared with their optimal values

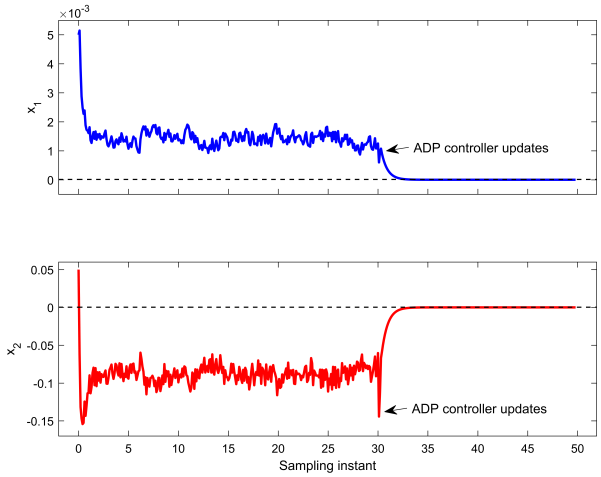

Fig. 4: System states with VI-based ADP control scheme

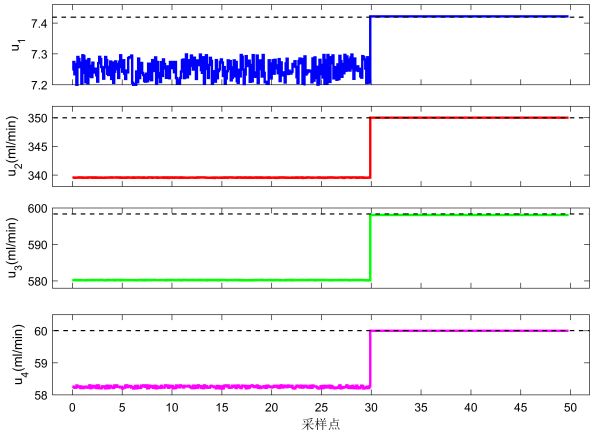

Fig. 5: Control inputs with VI-based ADP control scheme

4 Simulation result

In this section, the efficacy of the proposed VI-based ADP control approach is verified by numerical simulation. In order to model the reagents control in flotation process, we collect 4000 groups of reagent addition data and the corresponding 4000 groups of taling grade and concentrate grade data. In the flotation process model (29),

$$A_c = \begin{bmatrix} -11.6773 & -0.1531 \\ -1368.6 & -22.5954 \end{bmatrix},$$
$$B_{c1} = \begin{bmatrix} -0.1429 & 0 & 0 & 0 \\ -12.4712 & 0 & 0 & 0 \end{bmatrix},$$
$$B_{c2} = \begin{bmatrix} 0 & 0.0011 & 0 & 0 \\ 0 & -0.0567 & 0 & 0 \end{bmatrix},$$
$$B_{c3} = \begin{bmatrix} 0 & 0 & 0.00007 & 0 \\ 0 & 0 & 0.1613 & 0 \end{bmatrix},$$
$$B_{c4} = \begin{bmatrix} 0 & 0 & 0 & -0.0016 \\ 0 & 0 & 0 & -0.0491 \end{bmatrix},$$
$D_c = [0.3388, 18.8626]^T$.

The input time-delay is set to $\tau_1 = 0.03s$, $\tau_2 = 0.15s$, $\tau_3 = 0.25s$, $\tau_4 = 0.37s$, the sampling period is 0.1s, the weight matrix $Q = 10^{-5} I_{18}$, $R = I_4$. The optimal control gain K^* is obtained by calculating DARE (43) with matrix coefficients of the state space model.

Simulation has been carried out based on (34) and (35), where the exploration noise e_k is generated by the random generator. From Fig. 3, it can be seen that H_j and K_j iteratively learned from Algorithm 2 with industrial collected data converge to the optimal values H^* and K^* calculated by DARE with flotation process model after 14 iterations. Thus, the adaptive optimal controller $u_k = -Kz_k$ is obtained.

Then, the optimal control strategy learned from the Algorithm 2 is applied to the closed-loop system after $k = 30$, the following results are obtained: x_1 and x_2 converge to 0 with very small tracking error, as shown in Fig. 4. Meanwhile, Fig. 5 provides the recommended reagents addition $u = [u_1, u_2, u_3, u_4]$.

The significant advantage of the proposed method is its simplicity, which is independent of the precise knowledge of flotation dynamics with good disturbance rejection and fast setpoint tracking. The simulation demonstrated that the flotation process can be effectively controlled by the VI-based ADP algorithm.

5 Conclusions

In terms of input time-delay caused by the reagents reaction and material transfer, as well as the impacts of grinding process changes, a VI-based ADP algorithm is used to find a desirable adaptive optimal controller and implemented online using measurable data. In particular, an inner model is bring forward for compensating the external disturbance, and the optimal control action is derived by solving the Riccati equation with the proposed data-driven control policy. The simulation results show that the proposed ADP-based approach is suitable for minimizing the error between the flotation index and its reference, without the knowledge of system dynamics. In addition, the proposed learning-based technique can be easily extended to control other manipulated variables of the whole flotation plants, like pulp level and air inlet rate. These extension will be uncovered in later research.

References

[1] D. Su, Y. Su, D. H, and L. Yu, Analysis and outlook of economic situation of mineral resources in 2018, *Natural Resource Economics of China*, 32(1):30-35, 2019.

[2] M. Fuerstenau, G. Jameson, and R. Yoon, *Froth flotation: a century of innovation*. SME, 2007.

[3] T. Chai, L. Zhao, J. Qiu, F. Liu, and J. Fan, "Integrated network-based model predictive control for setpoints compensation in industrial processes," *IEEE Transactions on Industrial Informatics*, 9(1):417-426, 2013.

[4] D. Rojas, and A. Cipriano, "Model based predictive control of a rougher flotation circuit considering grade estimation in intermediate cells," *Dyna*, 78(166):29-37, 2011.

[5] A. Saravani, N. Mehrshad, and M. Massinaei, "Fuzzy-based modeling and control of an industrial flotation column," *Chemical Engineering Communications*, 201(7):896-908, 2014.

[6] J. Zhu, W. Gui, J. Liu, H. Xu, and C. Yang, "Combined fuzzy based feedforward and bubble size distribution based feedback control for reagent dosage in copper roughing process," *Journal of Process Control*, 39:50–63, 2016.

[7] E. Jorjani, S. Mesroghli, and S. C. Chelgani, "Prediction of operational parameters effect on coal flotation using artificial neural network," *Journal of University of Science and Technology Beijing, Mineral, Metallurgy, Material*, 15(5):528-533, 2008.

[8] E. Allahkarami, O. Salmani Nuri, A. Abdollahzadeh, B. Rezai, and B. Maghsoudi, "Improving estimation accuracy of metallurgical performance of industrial flotation process by using hybrid genetic algorithm–artificial neural network (gaann)," *Physicochemical Problems of Mineral Processing*, 53, 2017.

[9] Z. Li, and W. Gui, "The method of reagent control based on time series distribution of bubble size in a gold-antimony flotation process," *Asian Journal of Control*, 20(6):2223-2236, 2018.

[10] Y. Wang, B. Sun, R. Zhang, Q. Zhu, and F. Li, "Sulfur flotation performance recognition based on hierarchical classification of local dynamic and static froth features," *IEEE Access*, 6:14019-14029, 2018.

[11] F. Cubillos and E. Lima, "Identification and optimizing control of a rougher flotation circuit using an adaptable hybrid-neural model," *Minerals Engineering*, 10(7):707-721, 1997.

[12] B. Cao, Y. Xie, W. Gui, C. Yang, and J. Li, "Coordinated optimization setting of reagent dosages in roughing-scavenging process of antimony flotation," *Journal of Central South University*, 25(1):95-106, 2018.

[13] J. Li, T. Chai, F. L. Lewis, J. Fan, Z. Ding, and J. Ding, "Off-policy q-learning: Set-point design for optimizing dual-rate rougher flotation operational processes," *IEEE Transactions on Industrial Electronics*, 65(5):4092-4102, 2018.

[14] Y. Jiang, J. Fan, T. Chai, and F. L. Lewis, "Dual-rate operational optimal control for flotation industrial process with unknown operational model," *IEEE Transactions on Industrial Electronics*, 66(6):4587-4599, 2019.

[15] F. L. Lewis and D. Liu, *Reinforcement learning and approximate dynamic programming for feedback control*, John Wiley & Sons, 2013.

[16] D. Liu, Q. Wei, D. Wang, X. Yang, and H. Li, *Adaptive dynamic programming with applications in optimal control*. Springer, 2017.

[17] H. Zhang, D. Liu, Y. Luo, and D. Wang, *Adaptive dynamic programming for control: algorithms and stability*. Springer Science & Business Media, 2012.

[18] Y. Jiang, and Z.-P. Jiang, *Robust adaptive dynamic programming*. John Wiley & Sons, 2017.

[19] Q. Wei, and D. Liu, "Data-driven neuro-optimal temperature control of water–gas shift reaction using stable iterative adaptive dynamic programming," *IEEE Transactions on Industrial Electronics*, 61(11):6399-6408, 2014.

[20] X. Yang, H. He, and X. Zhong, "Adaptive dynamic programming for robust regulation and its application to power systems," *IEEE Transactions on Industrial Electronics*, 65(7):5722-5732, 2018.

[21] M. Huang, W. Gao, and Z.-P. Jiang, "Connected cruise control with delayed feedback and disturbance: An adaptive dynamic programming approach," *International Journal of Adaptive Control and Signal Processing*, 33(2):356-370, 2019.

[22] B. Pang, T. Bian, and Z.-P. Jiang, "Adaptive dynamic programming for finite-horizon optimal control of linear time-varying discrete-time systems," *Control Theory and Technology*, 17:73-84, 2019.

[23] O. Bascur, "On the development of a model-based control strategy for copper-ore flotation," *Flotation of Sulphide Minerals*, 409-431, 1984.

[24] R. BASCUR, "Modeling and computer control of a flotation cell.," 1983.

[25] M. Vera, J. Franzidis, and E. Manlapig, "Simultaneous determination of collection zone rate constant and froth zone recovery in a mechanical flotation environment," *Minerals Engineering*, 12(10):1163-1176, 1999.

[26] R. Honaker, M. Mohanty, and J. Crelling, "Coal maceral separation using column flotation," *Minerals Engineering*, 9(4):449-464, 1996.

[27] G. Bartolacci, P. Pelletier Jr, J. Tessier Jr, C. Duchesne, P.-A. Bossé, and J. Fournier, "Application of numerical image analysis to process diagnosis and physical parameter measurement in mineral processesłpart i: flotation control based on froth textural characteristics," *Minerals Engineering*, 19(6-8):734-747, 2006.

[28] M. Vera, Z. Mathe, J.-P. Franzidis, M. Harris, E. Manlapig, and C. O'Connor, "The modelling of froth zone recovery in batch and continuously operated laboratory flotation cells," *International Journal of Mineral Processing*, 64(2-3):135-151, 2002.

[29] Z. Mathe, M. Harris, and C. O'Connor, "A review of methods to model the froth phase in non-steady state flotation systems," *Minerals Engineering*, 13(2):127–140, 2000.

[30] K. J. Åström and B. Wittenmark, *Computer-controlled systems: theory and design*. Courier Corporation, 2013.

[31] J. Huang, *Nonlinear output regulation: theory and applications*, Siam, 2004.

[32] F. L. Lewis, D. Vrabie, and V. L. Syrmos, *Optimal control*. John Wiley & Sons, 2012.

[33] P. Lancaster, and L. Rodman, *Algebraic riccati equations*. Clarendon press, 1995.

[34] W. Gao, Y. Jiang, Z.-P. Jiang, and T. Chai, "Output-feedback adaptive optimal control of interconnected systems based on robust adaptive dynamic programming," *Automatica*, 72:37-45, 2016.